

## CFD Analysis of Fluid Flow through Reconstructed Metal Foams

S.T.W. Kuruneru<sup>1</sup>, D. Holmes<sup>1</sup>, S. Park<sup>1</sup>, E. Sauret<sup>1</sup>, Y.T. Gu<sup>1</sup>

<sup>1</sup>School of Chemistry, Physics, & Mechanical Engineering, Science and Engineering Faculty  
Queensland University of Technology, Brisbane, Queensland, 4000, Australia

### Abstract

The global energy demand signifies the importance of developing cutting-edge and state of the art heat exchanger technologies. The deployment of porous metal foams in various heat exchangers is one such material that is rapidly gaining attention in the research field. However, an in-depth comparative analysis of fluid flow through metal foams is relatively scarce in the existing literature. This study aims to use computational fluid dynamics (CFD) to examine forced convection of various fluids through digitized samples of porous metal foams. Results have shown that an increase in fluid velocity results in a decline in average fluid temperature. Moreover, the type of fluid has a direct effect on the temperature distribution and spread of the fluid temperature around the foam ligaments. This study aims to address critical queries in the literature namely unravelling forced convection of fluids through metal foams for compact and lightweight heat exchangers. This could potentially serve as a steppingstone to devise ways of mitigating fouling and maximizing heat exchanger performance.

### Introduction

Heat exchangers are omnipresent in a myriad of industrial applications such as power generation, oil refineries, dairy industry, among others. The global heat exchanger market is projected to reach US \$ 78.16 billion by 2020 [2]. The global energy demand will increase by almost 35 % by 2030; however, this can be as high as 95 % in the event energy efficient technologies are not utilized [4]. Also, small and lightweight heat exchangers utilising high energy consumption are increasingly being sought for compact heat sinks. Therefore, it is very important to develop energy efficient and effective heat exchange technologies to meet the global energy demand while ensuring that the introduction of novel heat exchange technologies does not compromise the global environment.

Metal foams are a viable alternative to conventional fin-based heat exchangers due to their superior thermo-physical properties such as high surface area to volume ratio, low weight, and good thermal conductance, among others. The stochastic and highly irregular geometric morphology of metal foams coupled with the very high surface area to volume ratio infer a high incidence of fluid mixing thereby amplifying turbulence and heat transfer [7]. Mahdi et al. [9] has shown that retrofitting highly porous metal foam inserts in a central processing unit (CPUs), with water as the coolant, yields a 70 % lower thermal resistance compared to fin-based CPU heat exchangers. Metal foams are also gaining attention in waste heat recovery applications. For instance, a recent study by Wang et al. [15] inferred that the maximum power generation of a thermoelectric generator (TEG) embedded with metal foams showed a 30 % increase as compared to a TEG without a metal foam insert, with air as the coolant. Alvandifar et al. [3] concluded that the same Nusselt number is realized when either a partially wrapped metal foams or full wrapped metal foams are used for air-cooled heat exchangers, in addition, a 60 % pressure drop is achieved with the use of a partially wrapped metal foam. Negligence of addressing critical thermal

management best practices could potentially degrade heat exchanger performance such as lower operational efficiency, longevity, and overheating of compact chips. Abadi et al. [1] experimentally investigated heat transfer and pressure drop in a metal foam-filled small tube (*i.e.* 4 mm diameter) air-cooled heat exchanger. It was found that the heat transfer coefficient increases significantly with increasing Reynolds number and the pores per inch (ppi) of a metal foam. The heat transfer coefficient of such systems is significantly greater than a tube with any metal foam inserts. Moreover, various new correlations have been proposed the discussion is not repeated here and the interested reader is referred to [1]. Interestingly, Dai et al. [6] used the  $\epsilon$ -NTU method to compare the performance of a flat-tube serpentine louver-fin heat exchanger to that of a flat-tube metal-foam heat exchanger subject to the same thermal-hydraulic requirements based on air as the working fluid. Results have shown that similar heat exchanger performance is achieved but the metal-foam system is significantly lighter and smaller. Nawaz et al. [11] investigated thermal hydraulic performance of air-cooled metal foam heat exchangers under dry operating conditions. One of the main findings is that foams with a smaller pore size (*i.e.* corresponding to 40 PPI) have a higher heat transfer coefficient as compared to larger pore size metal foams (5 PPI).

Clearly, the use of metal foams results in superior heat exchanger performance. However, a comparative analysis of temperature and velocity profiles based on different fluids (*i.e.* air, water) and different metal foam temperatures is severely lacking in the existing literature. The majority of studies are based on air which is suitable for heat exchangers in arid regions where water is scarce. However, the effects of heat transfer through metal foam heat exchangers based on water as the coolant is not thoroughly established in the existing literature. In addition, there exists no comparative heat transfer study between two different coolant fluids namely, air and water. It is noted that very few studies delved into multiphase solid-gas flows and fouling in metal foam heat exchangers. However, these studies used idealized metal foam geometries [8]. Also, all these studies are based on air as the working fluid. Therefore, the aim of this paper is to numerically investigate non-isothermal fluid flows through a metal foam structure based on X-ray micro-computed tomography ( $\mu$ -CT) imagery of a real metal foam sample. A pore-level analysis of fluid flow is conducted. Two different working fluids are investigated namely, air and water. The effects of various wall temperatures and fluid inlet velocities on the heat transfer profiles are investigated. In this research, non-isothermal single-phase fluid flow through real metal foams is assessed. This analysis serves as a steppingstone to address the thermal performance of foam heat exchanger designs for electronics cooling and heating, ventilation, air-conditioning, and refrigeration (HVAC&R) systems. This paper could potentially pave way for further studies in the near future such as reducing fouling and maintenance costs for metal foam heat exchangers.

## Numerical Model and Computational Domain

The transport of incompressible fluid through metal foams at the pore-level is governed by Navier–Stokes equations and is given by [10],

$$\frac{\partial}{\partial x_i} u_i = 0 \quad (1)$$

$$\frac{\partial}{\partial x_i} (\rho_f u_i u_j) = -\frac{\partial P}{\partial x_i} + \frac{\partial}{\partial x_i} \left( \mu_f \frac{\partial u_i}{\partial x_j} \right) \quad (2)$$

$$\frac{\partial}{\partial x_i} (\rho_f u_i c_p T) = \frac{\partial}{\partial x_i} \left( \lambda \frac{\partial T}{\partial x_i} \right) \quad (3)$$

where fluid density is denoted as  $\rho_f$ , fluid velocity  $u$ , fluid temperature  $T$ , fluid thermal conductivity  $\lambda$ , fluid dynamic viscosity  $\mu_f$ , specific heat capacity  $c_p$ , pressure  $P$ . The steady-state simulations are run in ANSYS Fluent [5], a commercial CFD program. The solution of the Navier–Stokes equations is obtained using the finite volume method (FVM). The Semi-Implicit Method for Pressure Linked Equations (SIMPLE) algorithm is deployed for pressure-velocity coupling. A second order upwind scheme is used for the momentum and energy spatial discretization. An under-relaxation factor of 0.7 and 1.0 is used for the momentum and energy terms respectively. The solution is initialized from the inlet at a known superficial inlet velocity, and the simulation is run until the convergence criteria for the residuals is reached which is  $1 \times 10^{-5}$  for the pressure and velocity and  $1 \times 10^{-6}$  for the energy. Several assumptions are made in this investigation. Firstly, the working fluid considered in this study is assumed incompressible. Secondly, radiation effects are neglected as the temperatures considered in this study is less than 700 K. Thirdly, the effect of particulate fouling on heat transfer performance is neglected for simplicity.

### Computational Domain

In this study, single-phase fluid flows and forced convection of fluids through an X-ray  $\mu$ -CT reconstructed metal foam geometry is investigated. Hereon, aluminium foam metal with a 20 pore per inch 6-8 % density 6101 alloy is used (ERG aerospace). The fibre ligament thickness or strut diameter is 0.20 mm. The goal of this study is to obtain a reconstructed metal foam specimen via X-ray  $\mu$ -CT and then to investigate forced convection of fluids at the pore-level as a first step to understanding the temperature profiles prior to moving to complex simulations such as multiphase solid-gas flows. Secondly, performing a full computational analysis of fluid flow of the entire macroscopic model, as shown in figure 1a, is extremely computationally demanding and difficult to solve using existing computing resources. As such, we restrict our attention to a small unit cell of dimensions  $3 \text{ mm} \times 3 \text{ mm} \times 4 \text{ mm}$ , as shown in figure 1b, which is the computational domain used in this study. Several authors have used a small portion or a representative elementary volume (REV) to represent the entire foam structure where the REV must be larger than the pore diameter but smaller than the macroscopic length of the entire foam geometry [14]. The following boundary conditions are assigned: inlet velocity, pressure outlet, symmetry walls around the lateral faces of the domain (dashed lines shown in figure 1b), and no-slip wall applied to the metal foam geometry.

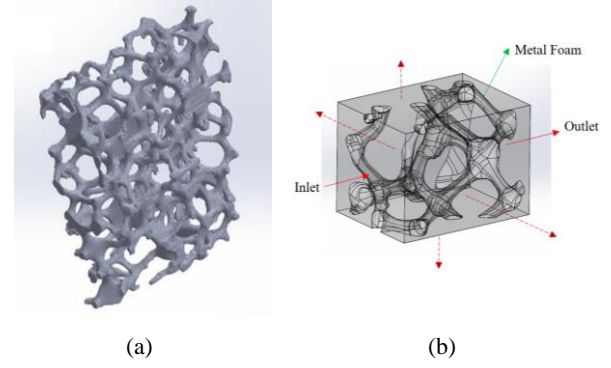


Figure 1. (a) Digitized scan of metal foam scans (DICOM) (b) representative elementary volume of metal foam structure.

In this study, various inlet velocities  $V_{in}$  are studied: 0.1 m/s and 0.3 m/s. Such velocities are found in HVAC&R systems. Two different working fluids are investigated in this paper: water and air. The fluid is injected along the inlet plane (*c.f.* figure 1b). Additionally, the temperature profiles of the foams based on various wall temperatures  $T_w$  are studied. The full list of case studies are shown in Table 1. It is noted that the fluid inlet temperature in all cases is 298 K. The Reynolds number, based on the strut diameter as the characteristic length and the inlet velocities considered in this study, ranges from 0.03 to 4.3.

### Metal foam reconstruction

X-ray  $\mu$ -CT is an imaging method used to obtain 3D reconstruction of an object in different directions. The visualization and analysis of the pores of the metal foams at a very small at high resolution is achieved using this technique. 3D volume renderings are created by the CT software to reconstruct the CT slices. The 3D volume comprises voxels which indicates an intensity value of a signal or colour in 3D space. The raw digitized scans are imported as a series of images as DICOM files. A series of operations is performed (region of interest, projection, binary tool, image scaling, plugin such as texture-based volume renderings) to obtain the surface images of the DICOM files. The  $\mu$ -CT data is processed using custom threshold and surface recognition software to produce a manifold triangular mesh surface and saved in STL format. This file then underwent mesh facet reduction, smoothing, and conversion from triangular to quadrilateral mesh to facilitate translation to a parametric surface in subsequent operations. A NURBS surface recognition is then carried out, and subsequent stitching and repair of the parametric surfaces performed to produce a parametric solid for final sample editing within any commercial solid modelling package or pre-processor. The rectangular cuboid encapsulating the metal foam ligaments, as shown in figure 1b, represents the fluid volume. This cuboid is designed in solidworks [12].

Case	Wall temperature $T_w$ [K]	Fluid Inlet velocity $V_{in}$ [m/s]
A (air) D (water)	310	0.10
B (air) E (water)	320	0.10
C (air) F (water)	330	0.10
M (air) P (water)	310	0.30
N (air) Q (water)	320	0.30
O (air) R (water)	330	0.30

Table 1 Case studies.

## Mesh Sensitivity Analysis

A mesh sensitivity analysis is performed. In this study, unstructured tetrahedral mesh is used. The criteria for the converged mesh is achieved when the global pressure drop between successive mesh refinements is less than 5%. Also, the local temperature profiles along a specific plane for each mesh refinement is recorded. The inlet velocity and wall temperature of this case is respectively, 0.10 m/s and 320 K, and the working fluid is air, corresponding to Case B.

Grid	Number of nodes [-]	Pressure Drop [Pa]
1	134571	3.44
2	210677	3.98
3	298404	4.17

Table 2 Pressure drop variation- Case B.

As shown in Table 2, the pressure drop remains almost invariant with increasing number of nodes with less than 5% difference in pressure drop between Grid 2 and Grid 3. As such, to ease computational burden, Grid 2 is selected for the remaining studies. An example of the temperature profile of the fluid based on Grid 2 is shown in figure 2. Moreover, the temperature variation of the fluid across a horizontal line located along the mid-section of the plane (*c.f.* figure 2b) is shown in figure 3. Clearly, no changes in temperature difference is observed regardless of the mesh quality.

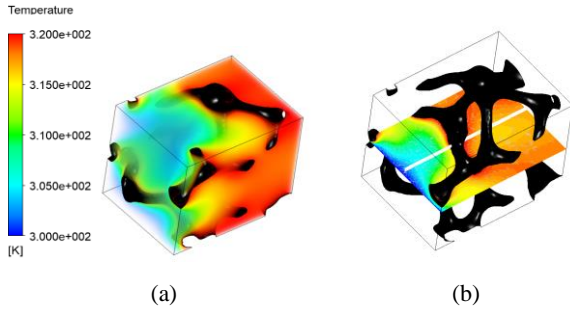


Figure 2 (a) Case B: volume renderings of temperature (b) local temperature profile extracted along a plane (note horizontal line drawn across the mid-section of the contour plot). Direction of flow from left to right.

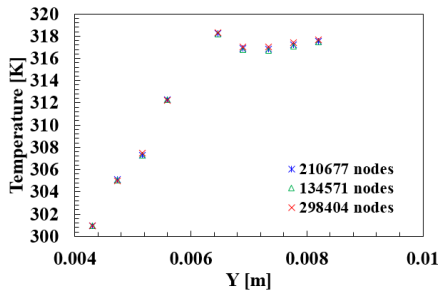


Figure 3 Temperature profiles along the horizontal line based on different mesh qualities corresponding to Case B.

## Results & Discussion

The temperature profiles of the working fluids based on various inlet velocities and foam wall temperatures is studied. We also examine the local temperature profiles extracted along the mid-section of the plane to provide a comprehensive view of temperature variation throughout the longitudinal axis (*c.f.* figure 2b). The volume renderings of the temperature which connote the global temperature profiles based on two different working fluids corresponding to  $V_{in} = 0.10$  m/s and  $T_w = 320$  K are shown in figure 4a & 4b. It is clearly shown that the working fluid has profound implications on the temperature and velocity patterns. The front and rear of the metal foam specimen has some clear temperature differences. In Case B, where the fluid

is air, the rear of the foam shows a wider area of high temperature hotspot as compared to Case E where water is the working fluid. In Case E, it is clearly observed that the foam wall temperature is slightly lower than the case with air (Case B). Water as the working fluid has a greater tendency to dissipate heat away from the metal foam structure. According to figure 5, the wakes at the rear of the foam in Case E (water) is slightly wider than the wakes observed in Case B (air). The metal foam ligaments impede the incoming fluid and due to the highly irregular and stochastic orientation of this foam, promote mixing of fluid. In both cases, the high temperature profiles located behind the struts of the foam (*c.f.* figure 4) infer stagnant zones of zero fluid velocity (*c.f.* figure 5). The average fluid temperature  $T_{ave}$ , of Case B and Case E is, respectively, 317 K and 306 K, which is lower than the maximum fluid temperature (320 K) due to the fluid mixing caused by these stochastic foam structures.

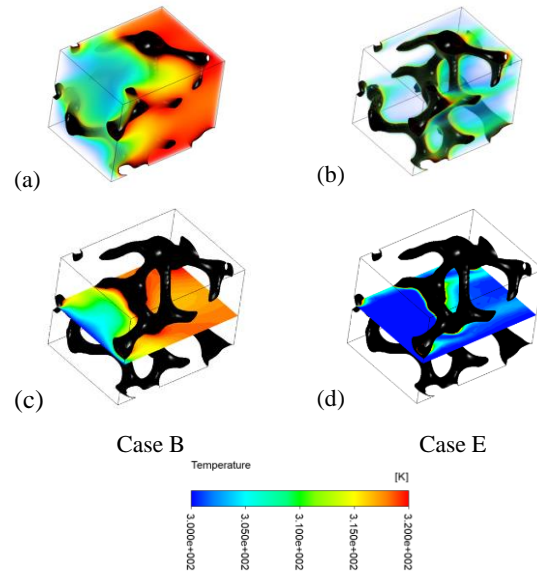


Figure 4. Fluid temperature profiles at  $T_w = 320$  K and  $V_{in} = 0.10$  m/s based on air (Case B) and water (Case E). Direction of fluid flow from left to right.

The fluid vortices are clearly observed in Case E where the working fluid is water. No vortices were observed in Case B. Vortices for Case E are observed in two zones: Zone 1 and Zone 2, a close up view of the recirculation regions are shown in figure 6. Interestingly, recirculation is not observed in any of the air coolant cases regardless of inlet velocities. The local temperature profiles is extracted along the horizontal line located in the mid-section of the plane (*c.f.* figure 2) and the results are shown in figure 7. The temperature profiles are based from  $\sim 0.0042$  m which is located at the inlet plane up towards the outlet plane located at  $\sim 0.0085$  m along the y-axis.

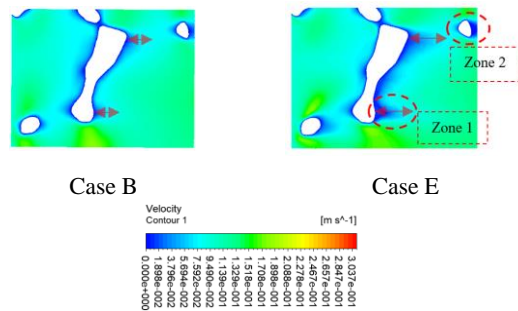


Figure 5. Fluid velocity profiles extracted along the mid-section plane of the foam for  $T_w = 320$  K and  $V_{in} = 0.10$  m/s. Direction of flow from left to right.

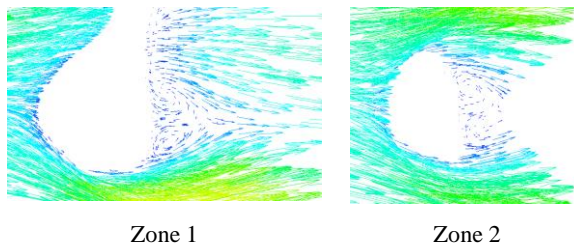


Figure 6. Close-up view of fluid vortices corresponding to Case E.

It is clearly shown that the temperature of the fluid increases along the streamwise direction. According to figure 7a, the fluid temperature increases with increasing wall temperature under the same inlet velocity ( $V_{in} = 0.10$  m/s). Interestingly, the rear of the foam ( $Y > 0.006$  m) exhibit nearly no significant temperature variation compared to the front ( $Y < 0.006$  m). Also, according to figure 6c, the fluid temperature at the front of the foam is nearly identical, whereas the rear of the foam showed significant difference; however, this discrepancy reduces substantially towards the outlet plane (*i.e.*  $Y \rightarrow 0.008$  m). A similar observation is realized at  $V_{in} = 0.30$  m/s, as shown in figure 6b & 6d. Clearly, the maximum fluid temperature corresponding to all water cases is lower than all cases based on air. All cases show a lower local temperature distribution with increasing inlet velocity. This is because at higher inlet velocities, the fluid dissipates heat at a rapid rate as compared to cases at lower inlet velocities. The Prandtl number  $Pr$  of the fluids vary: 6.15 for water and 0.66 for air. The  $Pr$  is expressed as a function of the fluid specific heat capacity, dynamic viscosity, and thermal conductivity; essentially the ratio of momentum diffusivity to thermal diffusivity. The thermal conductivity of water and air is, respectively, 0.608 W/m-K and 0.026 W/m-K. Heat diffuses more slowly in water than air because an increase in  $Pr$  means that heat diffuses more slowly thereby explaining the lower temperature profiles of the case with water. The next phase of this research is to account for multiphase solid-gas flows as it would be interesting to visualize the solid particle interactions with the fluid recirculation regions (*c.f.* figure 6).

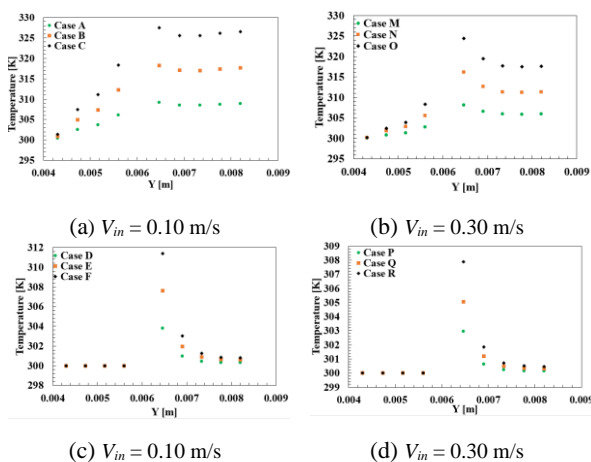


Figure 7. Local temperature profiles along mid-section based on two different fluids: air (a-b) and water (c-d).

## Conclusions

The temperature profiles of single-phase fluid flows through metal foams reconstructed by X-ray  $\mu$ -CT scan is examined. Two working fluids, inlet velocities, and wall temperatures are studied. An increase in inlet velocity showed a decrease in average fluid temperature; fluid wakes are localized around the foam ligaments where temperature hotspots are present. As far as the authors know, there is no experimental data pertaining to this exact same heated metal foam specimen (*i.e.* based on the

same fibre thickness, porosity, cell diameter) immersed in water and air. However, experimental analysis is to be conducted to compare against numerical results in the foreseeable future. It is noted that the authors conducted validation works based on similar models [8]. Certain industrial applications, such as heat exchangers, comprise multiphase flows and particulate fouling [13]. As such, the next phase of this research is to study transient multiphase solid-gas simulations and the effects of particulate fouling by using fully resolved simulations such as the coupled finite volume & discrete element method.

## References

- [1] Abadi, G.B., & Kim, K.C., Experimental heat transfer and pressure drop in a metal-foam-filled tube heat exchanger, *Exp. Ther. & Fluid Science*, **82**, 2017, 42-49.
- [2] Acmite, *Global heat exchanger market report*, Tech. Rep, 2013.
- [3] Alvandifar, N., Saffar-Avval, M., & Amani, E., Partially metal foam wrapped tube bundle as a novel generation of air-cooled heat exchangers, *In. J. Heat & Mass Transfer*, **118**, 2018, 171-181.
- [4] Ammar, Y. J., Low grade thermal energy sources and uses from the process industry in the UK, *Applied Energy*, **89**, 2012, 3-20.
- [5] ANSYS (R) [ANSYS Fluent] *Academic Research*, Release 19, 2018.
- [6] Dai, Z., Nawaz, K., Park, Y., Chen, Q., & Jacobi, A., A Comparison of Metal-Foam Heat Exchangers to Compact Multilouver Designs for Air-Side Heat Transfer Applications, *Heat Transfer Engineering*, **33**, 2012, 21-30
- [7] Han, X., Wang, Q., Park, Y., T'Joen, C., Sommers, A., & Jacobi, A., A review of metal foam and metal matrix composites for heat exchangers and heat sinks, *Heat Transfer Engineering*, **33**, 2012, 991-1009.
- [8] Kuruneru, S.T.W., Sauret, E., Saha, S.C., & Gu, Y., Numerical investigation of the temporal evolution of particulate fouling in metal foams for air-cooled heat exchangers, *Applied Energy*, **184**, 2016, 531-547.
- [9] Mahdi, H., Lopez, P., Fuentes, A., & Jones, R., Thermal performance of aluminium-foam CPU heat exchangers, *Int. J. of Energy Research*, **30**, 2006, 851-860.
- [10] Narsilio, G., Buzzi, O., Fityus, S., Yun, S., & Smith, D., Upscaling of Navier-Stokes equations in porous media: Theoretical, numerical and experimental approach, *Computers and Geotechnics*, **36**, 2009, 1200-1206.
- [11] Nawaz, K., Bock, J., & Jacobi, A., Thermal-hydraulic performance of metal foam heat exchangers under dry operating conditions, *App. Ther. Eng.*, **119**, 2017, 222-232
- [12] SolidWorks ® Education Edition, 2014 edition.
- [13] Traore, P. L., Laurentie, J.C., & Dascalescu, L., An efficient 4 way coupling CFD-DEM model for dense gas-solid particulate flows simulations, *Computers & Fluids*, **113**, 2015, 65-76.
- [14] Vafai, K. *Handbook of Porous Media*, 2<sup>nd</sup> edn. New York, Taylor & Francis, 2004.
- [15] Wang, T. L., Luan, W., Liu, T., Tu, S.T., & Yan, J., Performance enhancement of thermoelectric waste heat recovery system by using metal foam inserts, *Energy Conversion and Management*, **124**, 2016, 13-19.